

# Design and test of a dual-PRT scheme for the French radar network

P. Tabary, L. Périer, J. Gagneux, and J. Parent-du-Châtelet

Centre de Météorologie Radar, Direction des Systèmes d'Observation, Météo France, 7, rue Teisserenc-de-Bort, 78195 Trappes, France

**Abstract.** This paper describes the design and test of a staggered PRT scheme for the French radar network. The design of the staggered scheme has been done in the following context: 1) the scheme is meant to be implemented on existing C-band and S-band radars of the network, the PRF of which cannot, for technical reasons, be increased above their current values (300–400 Hz for C-band and 250–300 Hz for S-band); 2) the minimum expected Nyquist velocity should be around  $30 \text{ ms}^{-1}$ ; 3) the Doppler information will essentially be used to retrieve a VAD wind profile and for data assimilation by operational non hydrostatic numerical prediction models.

An operational C-band radar of the network, located in Trappes, near Paris, has been modified in July 2003 in order to allow Doppler processing and a dual-PRT staggered scheme with two low PRF ( $\text{PRF}_1=310$  and  $\text{PRF}_2=360$  Hz corresponding to a ratio of 6/7) has been implemented. Using two months of data (July–August 2003), the performance of the scheme is assessed qualitatively and quantitatively through the computation of the error structure of the various velocities: velocity at  $\text{PRF}_1$ , velocity at  $\text{PRF}_2$  and combined velocity. The error structure is obtained by using internally-generated, quality-checked VAD wind profiles as reference. The sensitivity of the error structure on the Signal Noise Ratio is also documented. A  $7 \times 7 \text{ km}^2$  median filter is introduced that significantly reduces dealiasing errors.

The efficiency of the scheme is finally evaluated indirectly by comparing the retrieved VAD wind profiles to external measurements such as co-located radiosoundings and model analyses.

## 1 Introduction

Dual-PRF (Pulse Repetition Frequency) Doppler schemes are now widely used among operational radar networks in order to increase the Nyquist velocity ( $V_N$ ) while keeping the

PRFs relatively low. Series of 32 or 64 pulses are used consecutively to estimate velocities at lag  $T_1$  ( $V_1$ ) and  $T_2$  ( $V_2$ ).  $V_1$  and  $V_2$  are combined in a second step to provide an unaliased radial velocity  $V$ . The advantage of dual-PRF schemes is that they allow performing FFT on the radar signal and filtering out the contribution of ground clutter. Its drawback however is that the two velocity estimates ( $V_1$  at lag  $T_1$  and  $V_2$  at lag  $T_2$ ) are not exactly representative of the same volume due to the fact that the antenna rotates during data collection. In presence of strong windshear, this can cause important errors in the dealiasing process (Joe and May, 2003; Holleman and Beekhuis, 2003).

Dual-PRT schemes on the other hand (Doviak and Zrnic, 1984; Zrnic and Mahapatra, 1985; Gray et al., 1989) that consist in alternating the PRF on a pulse-by-pulse basis do not induce such errors as the data used for estimating  $V_1$  and  $V_2$  are completely interleaved. Doppler spectrum estimation, though possible, is however getting more complex (Sachidananda and Zrnic, 2002).

The 18 radars of the French ARAMIS network are all conventional non-Doppler radars. A project is currently being run aiming at 1) renewing two ageing radars of the network (Trappes and Toulouse), 2) adding six more radars over the period 2004–2006 and 3) introducing new techniques such as volumic exploration, Doppler processing and polarimetry. In that context, an operational C-band radar of the network (Trappes, near Paris) has been modified and equipped with Doppler capacity. A staggered-PRT Doppler scheme has been designed and implemented on the radar in July 2003. Two months of data (July–August 2003) have been used to assess the feasibility of the scheme and compute the error distribution of the different velocities ( $V_1$ ,  $V_2$  and extended velocity  $V$ ). Results are detailed in Tabary et al. (2004) and thus only briefly recalled in Sect. 3. A VAD (Velocity Azimuth Display, Browning and Wexler 1968) wind profile algorithm has been used to generate wind profiles in real-time. The wind profiles have been compared to the French ARPEGE model analyses and to co-located radiosonde data. The comparison is described in Sect. 4. Section 5 finally gives the summary and the perspectives.

---

Correspondence to: P. Tabary  
(pierre.tabary@meteo.fr)

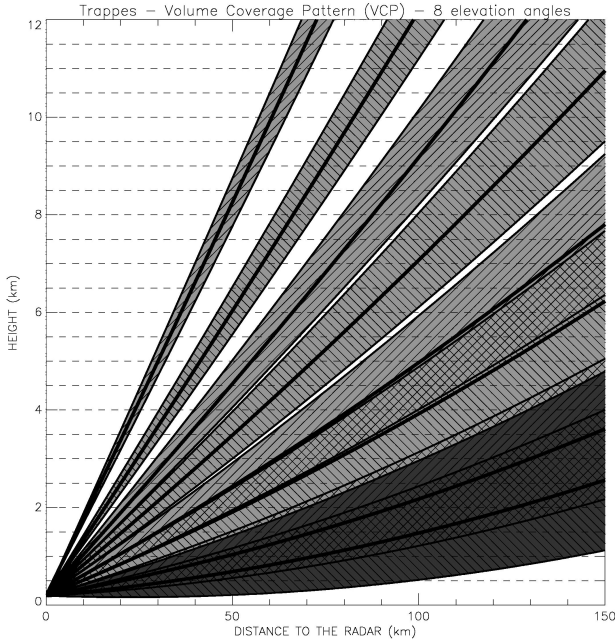


Fig. 1. VCP of the Trappes radar.

## 2 Design of the staggered scheme

The design of the scheme (Tabary et al., 2004) was done according to the following considerations:

The scheme is meant to be used for all radars of the network. As a consequence, it has to deal with low PRFs typically 333 Hz for C-band radars and 250 Hz for S-band radars.

The minimum extended Nyquist velocity ( $V_N$ ) should be around 30 m/s.

The radial velocity data will mainly be used for VAD wind profile retrieval and data assimilation. Ground-clutter identification is currently done quite efficiently by using the pulse-to-pulse fluctuation of the radar signal (Sugier et al., 2002).

Given the above-mentioned considerations, the two PRF were set to 360 Hz and 310 Hz, in a ratio of 6/7. The corresponding Nyquist velocities are equal to 4.1 m/s ( $V_{N1}$ ), 4.8 m/s ( $V_{N2}$ ) and 29.8 m/s ( $V_N$ ). The volume coverage pattern (VCP) of the Trappes radar is depicted on Fig. 1. The sampling cycle is such that 8 independent elevation angles are explored every 15 min. Among them, two are revisited every 5 min for hydrological purposes (0.4 and 0.8°). Cartesian ( $1 \text{ km}^2$ ,  $512 \times 512 \text{ km}^2$ ) images of reflectivity, velocity at lag  $T_1$  ( $V_1$ ), velocity at lag  $T_2$  ( $V_2$ ) and unaliased velocity ( $V$ ) for each elevation angle were generated in real-time and archived

It is worth at this point mentioning that the linear receiver of the radar was configured so as to make the noise level as low as possible to enhance the clear-air detection capability of the radar. Tabary et al. (2004) have shown that Doppler measurements were available 80% (resp. 70% and 35%) of the time during the warm season at 1000 m AGL (resp. 1500 and 2000).

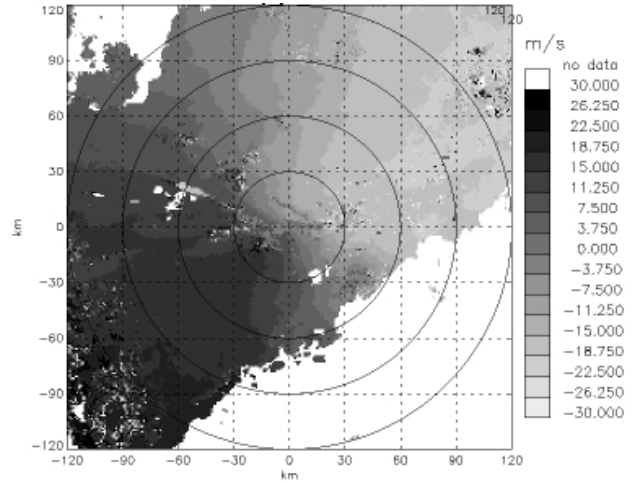


Fig. 2. Radial velocity PPI obtained for the 26 July 2003 17.15 UTC.

## 3 Evaluation of the consistency of the scheme

A first rather subjective way to evaluate the performance of the Doppler scheme is to examine the radial velocity maps and look at its consistency. Figure 2 shows the (extended) radial velocity map obtained at 17.15 UTC on the 26 July 2003 for the 0.4° elevation angle. A widespread precipitation system was starting passing over the radar at that time. The flow was mainly from the southwest with velocities up to 25 m/s (i.e. below the Nyquist threshold of 29.8 m/s). Some erroneous pixels are clearly visible in the southwest corner of the domain but also at closer ranges from the radar (e.g. along the 20-km range circle for instance). These outliers with respect to the background flow are consequences of dealiasing error.

In order to be a bit more specific about those dealiasing errors and to document the error structure of the extended radial velocity, the following methodology was developed:

A  $7 \times 7 \text{ km}^2$  median filter was applied to the extended radial velocity maps in order to remove outliers from the images. Figure 3 illustrates the effect of the median filter on the same situation as introduced before.

A VAD wind profile was retrieved every 15 min from the set of 12 median-filtered radial velocity maps gathered over the sampling cycle. The parameters of the wind profile retrieval method are detailed in Sect. 4.

The quality-checked VAD wind profiles were then used, wherever possible, to reconstruct radial velocity fields. Those radial velocity fields were then considered as reference maps against which the original, unfiltered, radial velocity maps could be compared. In that process, only velocities up to 30 km are used to make the VAD linearity assumption as valid as possible.

Error histograms were obtained by Tabary et al. (2004) for  $V_1$ ,  $V_2$  and  $V$  using two months of data (July–August 2003). Figure 4 shows the one obtained for  $V$ . The vertical scale is logarithmic and the error spans  $[-30; 30] \text{ m/s}$ .

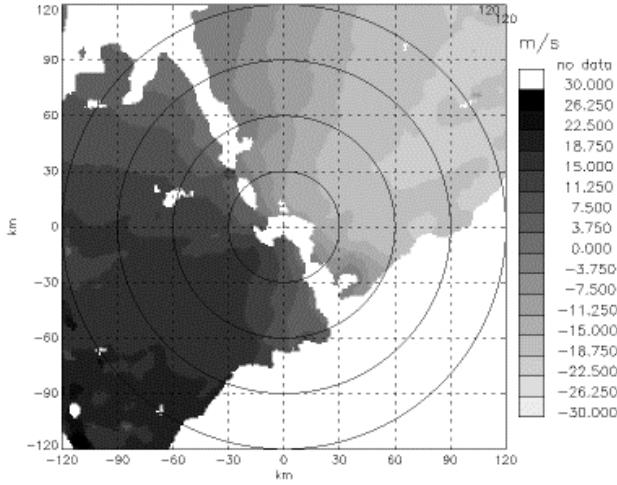


**Fig. 3.** Same as Fig. 2 but after application of a  $7 \times 7 \text{ km}^2$  median filter.

Whatever the SNR (Signal-Noise-Ratio) may be, the curve evidences a prominent maximum around zero with secondary and higher-order maxima. These maxima are shifted by  $\pm 2k.V_{N1}$  around zero, which means that they correspond to dealiasing errors. Consistently with theoretical results (Doviak and Zrnic, 1984), those secondary maxima decrease (exponentially) as the SNR increases.

Superimposed on the set of SNR-dependent error histograms on Fig. 4 is the error histogram obtained with the  $7 \times 7 \text{ km}^2$  median-filtered velocities. It can be clearly seen that the secondary maxima have been strongly reduced. This is just a more quantitative assessment of the “cleaning effect” of the median filter, already evidenced on Fig. 3. The width of the filter may appear a bit large but it should be kept in mind that those radial velocities will primarily be used for assimilation in numerical prediction models, the effective resolution of which is around 5 km. Tornadoes and other micro-scale phenomena are not so common in France so that spatial resolution is not really a key issue.

#### 4 Comparison of VAD wind profiles with model analyses and radiosonde data

As a further but indirect validation of the Doppler scheme, an evaluation of VAD wind profiles (Browning and Wexler, 1968) was carried out using model analyses on the one hand and radiosonde data on the other hand.

The  $u$  and  $v$  wind components were retrieved using the VVP method (Waldteufel and Corbin, 1979). The parameters of the retrieval are largely inspired from the study of Holleman (2003):

- The input data are the  $7 \times 7 \text{ km}^2$  median-filtered radial velocity maps;
- Ground-clutter pixels were rather crudely filtered out by removing all low-velocity pixels (less than 1 m/s);

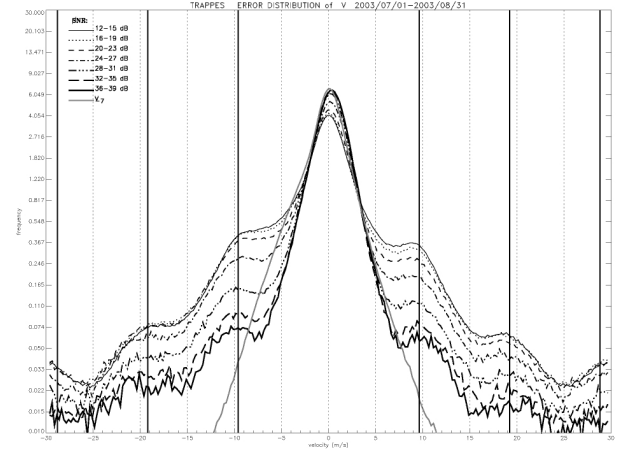


**Fig. 4.** Error distribution of the dealiased radial velocity for different values of the Signal-Noise-Ratio. The vertical axis is logarithmic and the error values span the range  $[-30, 30] \text{ m/s}^{-1}$ .

- Data at all elevation angles up to 30 km were considered in the analysis;
- The wind components were retrieved every 200 m between 0 and 5000 m through a least-square fit to the observed data. Higher-order terms of the VVP expansion were neglected;
- No data gap larger than  $120^\circ$  was tolerated along the azimuth in each 200 m layer;
- A quality control of the wind profile was performed afterwards based only on the number of points taken into account in the analysis. The dispersion around the sine curve was not used initially (see below).

Wind profiles were transmitted every 15 min in real time to Toulouse between the 17 February and the 14 March 2004 in order to be monitored by the French ARPEGE numerical prediction model. The monitoring is a continuous process that consists in checking the quality of incoming observations by comparing them to the model analyses. Biases and standard deviations are computed on a monthly basis. Observations that do not fulfill the quality requirements (expressed in terms of thresholds on the bias and standard deviation) are no longer assimilated by the model. In the present case, the Trappes VAD wind profiles were compared to model-analyzed wind profiles interpolated both in space and time. Figure 5 gives the results of the monitoring in terms of standard deviation and bias of the wind speed (left) and direction (right). Results are layered by altitude (between 0 and 5000 m ASL).

The number of available measurements in each layer is also shown on Fig. 5. The standard deviation of the wind speed difference is around 3 m/s, which is slightly worse than the score of the co-located Trappes radiosondes over the same period (2 m/s) but is still acceptable. The bias however appears to be positive at all levels, reaching a maximum of 2–3 m/s in the first 1000 m. Another maximum is to be seen

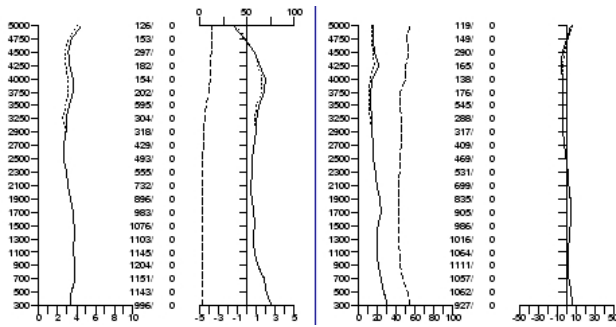


**Fig. 5.** Results of a 1-month monitoring by the French operational ARPEGE model. From left to right: vertical profiles of the standard deviation and mean value of the wind speed difference ( $\text{m s}^{-1}$ ) and standard deviation and mean value of the wind direction difference (degrees). The figures on the right of the standard deviation profiles indicate the number of couples used to compute the statistics for each layer.

higher in altitude at 4000 m but the number of available measurements (150) is probably not sufficient to make it statistically significant. The standard deviation of the wind direction difference (computed only over non-zero wind vectors) decreases steadily from 30 degrees at ground level down to 10 degrees at 5000 m, which is once again larger but close to the score obtained by the Trappes radiodondes. There is no bias in the wind direction at any level.

As a further evaluation, the algorithm was re-run on 7 months of data (July 2003–January 2004) leading to a total of more than 20 000 15-minute profiles. The 00 UTC and 12 UTC profiles were extracted from the data base to be compared with collocated radiosonde data. High-resolution radiosonde data were interpolated onto the same vertical grid as the VAD wind profiles. This led to a total of 2264 pairs of wind measurements. Some preliminary tests have shown that results were not sensitive to the time shift between radar and radiosonde measurements. Figures 6 and 7 show respectively the scatterplots of the wind speeds and directions measured by the radar (WR standing for Weather Radar and RS standing for Radiosounding). The bias, standard deviation, number of pairs of measurements and correlation coefficient are given in Figs. 6 and 7.

The 7-month period comparison does not reveal the same wind speed bias as was observed on Fig. 5 (results of the monitoring by the model). The standard deviation reaches 3.95 m/s and the correlation coefficient ( $R^2$ ) 0.68 which can clearly not be considered as excellent scores. Results for the wind direction are also contrasted with a slightly (unexplained) positive bias ( $5.2^\circ$ ), a standard deviation of  $33.4^\circ$  and a correlation coefficient of 0.89.

As mentioned before, the quality control only relied initially on the number of data points taken into account to retrieve the  $u$  and  $v$  wind components. Another useful parameter, pointed out by Holleman (2003), is the dispersion ( $\sigma$ ) around the sine curve once the retrieval has been done. If the dispersion is above a predetermined threshold – which can be caused either by non linearities in the wind

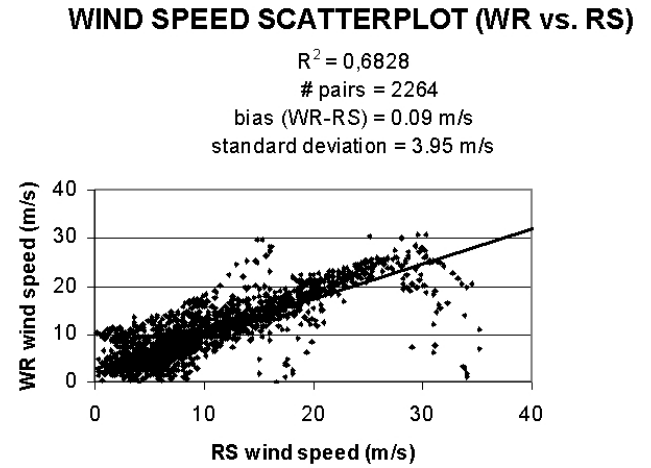


**Fig. 6.** Wind speed scatterplot (Weather Radar versus Radiosounding).

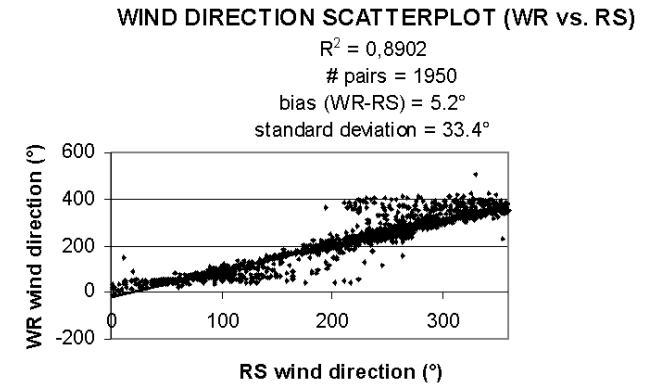


**Fig. 7.** Wind direction scatterplot (Weather Radar versus Radiosounding).

field or noisy data or velocity aliasing – then the corresponding wind vector is replaced by a missing data. Figures 8 and 9 show the same scatterplots as before (Figs. 6 and 7) but after introduction of an additional quality control based on  $\sigma$  ( $\sigma < 7 \text{ m/s}$ ).

As usual, the introduction of an additional quality control improves the scores but reduces the number of available measurements by about 40%. The standard deviation of the wind speed difference goes down to 2.8 m/s and the coefficient correlation increases up to 0.83. A good illustration of the effect of the quality check is the elimination of all the outliers that can be seen on Fig. 6 at large RS wind speeds. Such wind speeds were above the Nyquist threshold of the Doppler scheme (29.8 m/s) and presumably lead to aliased velocities and erroneous wind measurements. The bias in the wind direction is reduced to  $2.2^\circ$  and the standard deviation of the wind direction difference goes down to  $21^\circ$ . The correlation coefficient is now equal to 0.93.

Other sensitivity studies have been carried out to try and improve the tuning of the algorithm (e.g. the number of points included in the analysis, the maximum distance up to

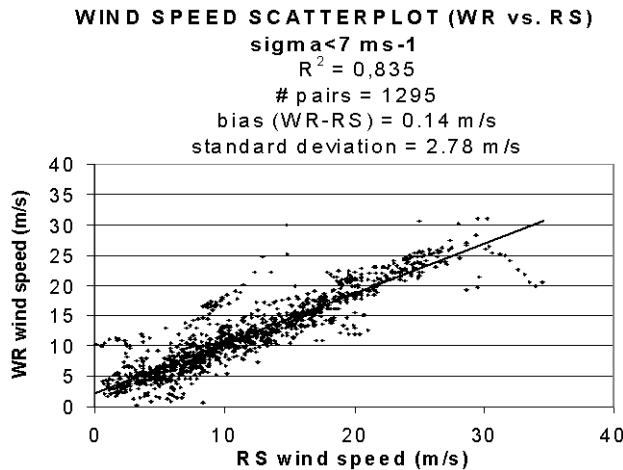


**Fig. 8.** Same as Fig. 6 but after introduction of a threshold on sigma ( $\sigma < 7 \text{ m/s}$ ).

which radial velocities are considered, elevation angles considered, ...) but none of them turned out to be as effective as sigma. As the wind profiles are meant to be used for data assimilation purposes, it has been decided to introduce the sigma-based quality control even though it induces a loss of about 40% of the wind measurements.

## 5 Summary and perspectives

In this paper, we have presented the test of a staggered PRT scheme that has been implemented on one operational C-band radar of the network. The scheme works with two rather low PRF in a ratio of 6/7. The individual and extended Nyquist velocities are equal to 4.1, 4.8 and 29.8 m/s.

The error distribution of the unaliased radial velocity has been computed using two months of data (July–August 2003) and quality checked VAD wind profiles. The error distribution evidences a main peak at zero but also secondary maxima shifted by  $\pm 2k \cdot V_{N1}$  around zero that can clearly be associated to dealiasing failures. The success rate of the dealiasing procedure increases with the Signal-Noise-Ratio. The application of a  $7 \times 7 \text{ km}^2$  median filter turns out to be very efficient to remove outliers in radial velocity maps.

A VAD wind profile algorithm has been implemented and the VAD wind profiles have been compared to model analyses over a 1-month period (17 February 2004–14 March 2004) and to radiosonde data over another 7-month period (July 2003–January 2004).

The VAD wind profiles are globally consistent with both model analyses and radiosonde data. The standard deviation is around 3–4 m/s for the wind speed and 10–20 degrees for the wind direction. The VAD wind speed is positively biased with respect to the model-analysed wind speeds but this bias is not confirmed by the long-term radar–radiosonde comparison.

A number of sensitivity tests have revealed that the most determining parameter in the VAD algorithm is the disper-

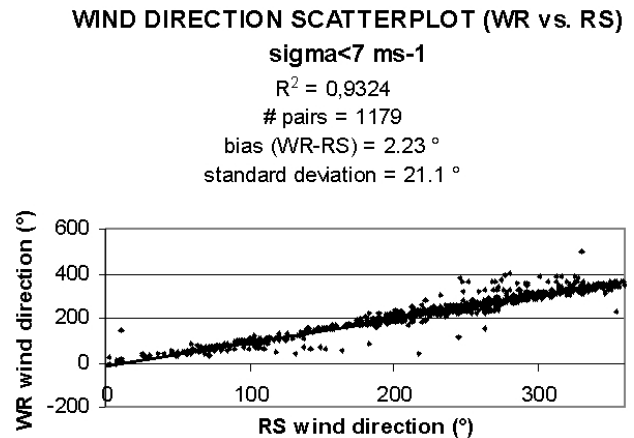


**Fig. 9.** Same as Fig. 7 but after introduction of a threshold on sigma ( $\sigma < 7 \text{ m/s}$ ).

sion around the sine curve. Introducing a threshold of 7 m/s on sigma significantly improves the quality of the VAD wind profiles.

## References

- Browning, K. A. and Wexler, R.: The determination of kinematic properties of a wind field using Doppler radar, *J. Appl. Meteor.*, 7, 105–113, 1968.
- Doviak, R. J. and Zrnic, D. S.: Doppler radar and weather observations, Academic Press Inc., 458 pp, 1984.
- Gray, G., Lewis, B., Vinson, J., and Pratte, F.: A Real-Time Implementation of Staggered PRT Velocity Unfolding, *Journal of Atmospheric and Oceanic Technology*, 6, No. 1, pp. 186–187, 1989.
- Holleman, I.: Quality of weather radar wind profiles, *Proceedings of the 31st Conference on Radar Meteorology*, 6–12 Aug. 2003, Seattle, WA, USA, 2003.
- Holleman, I. and Beekhuis, H.: Analysis and correction of dual-PRF velocity data, *J. Atmos. Ocean. Technol.*, 20, pp 443–453, 2003.
- Joe, P. and May, P. T.: Correction of Dual PRF Velocity Errors for Operational Doppler Weather Radars, *J. Atmos. Oceanic Technol.*, 20, No. 4, pp. 429–442, 2003.
- Sachidananda, M. and Zrnic, D. S.: An Improved Clutter Filtering and Spectral Moment Estimation Algorithm for Staggered PRT Sequences, *J. Atmos. Oceanic Technol.*, 19, No. 12, pp. 2009–2019, 2002.
- Sugier, J., Parent-du-Châtelet, J., Roquain, P. and Smith, A.: Detection and removal of clutter and anaprop in radar data using a statistical scheme based on echo fluctuation. *Proceedings of the Second European Radar Conference*, Delft, the Netherlands, 2002.
- Tabary, P., Périer, L., Gagneux, J., and Parent-du-Chatelet, J.: Test of a staggered PRT scheme for the French radar network, *J. Atmos. Oceanic Technol.*, in revision, 2004.
- Waldteufel, P., and Corbin, H.: On the analysis of single Doppler radar data, *J. Appl. Met.*, 18, pp 534–542.
- Zrnic, D. S. and Mahapatra, P.: Two methods of ambiguity resolution in pulse Doppler weather radars, *IEEE Trans. Aerospace and Electronic Systems*, AES 21(4), 470–483, 1985.